# GOODS-ALMA: AGNs and the slow downfall of massive star-forming galaxies at $z > 2$

## Maximilien Franco[1,2]

[1]AIM, CEA, CNRS, Université Paris-Saclay, Université Paris Diderot, Sorbonne Paris Cité, F-91191 Gif-sur-Yvette, France

[2]Centre for Astrophysics Research, University of Hertfordshire, Hatfield, AL10 9AB, UK
email: m.franco@herts.ac.uk

**Abstract.** We present the results of a 69 arcmin$^2$ ALMA survey at 1.1 mm, GOODS-ALMA, matching the deepest HST-WFC3 H-band observed region of the GOODS-South field. The 35 galaxies detected by ALMA are among the most massive galaxies at $z = 2-4$ and are either starburst or located in the upper part of the galaxy star-forming main sequence. The analysis of the gas fraction, depletion time, X-ray luminosity and the size suggests that they are building compact bulges and are the ideal progenitors of compact passive galaxies at $z \sim 2$, and a slow downfall scenario is favoured in their future transition from star-forming to passive galaxies.

**Keywords.** galaxies: evolution, galaxies: high-redshift, galaxies: ISM, galaxies: nuclei, submillimeter

## 1. Introduction

The star-formation density at high-redshift remains relatively unknown. For galaxies located beyond the peak of the star formation rate (SFR) density ($z \sim 2$; Madau & Dickinson 2014), their SFRs are commonly estimated from UV measurements. Since the UV emission is highly sensitive to dust attenuation, these SFRs must be corrected to obtain the effective star formation rate. For this purpose an extinction law (e.g., Meurer *et al.* 1999; Calzetti *et al.* 2000) and a UV spectral slope ($\beta$) has been calibrated in the local universe. Several caveats persist at high redshift (e.g., Cowie *et al.* 1996; Pannella *et al.* 2009), especially for galaxies with high SFRs (e.g., Rodighiero *et al.* 2011), making the estimation of intrinsic SFR in high redshift galaxies highly uncertain.

It is for this reason that the observation of galaxies at infrared wavelengths through large surveys is essential to understand how galaxies build up their stellar mass across cosmic time. The millimetre and submillimetre wavelengths, benefiting from a strong negative K-correction across a wide redshift range $2 < z < 10$ (e.g., Blain *et al.* 2002), are particularly well-suited for probing high redshift dust-obscured star formation.

The advent of the Atacama Large Millimetre/submillimetre Array (ALMA) has led to a considerable improvement in the angular resolution and sensitivity of the detections. We present here the results of the largest survey obtained with ALMA, GOODS-ALMA, covering 69 arcmin$^2$ in the deepest part of Cosmic Assembly Near-infrared Deep Extragalactic Legacy Survey (CANDELS; Koekemoer *et al.* 2011; Grogin *et al.* 2011) field, within the Great Observatories Origins Deep Survey-South (GOODS-South) field.

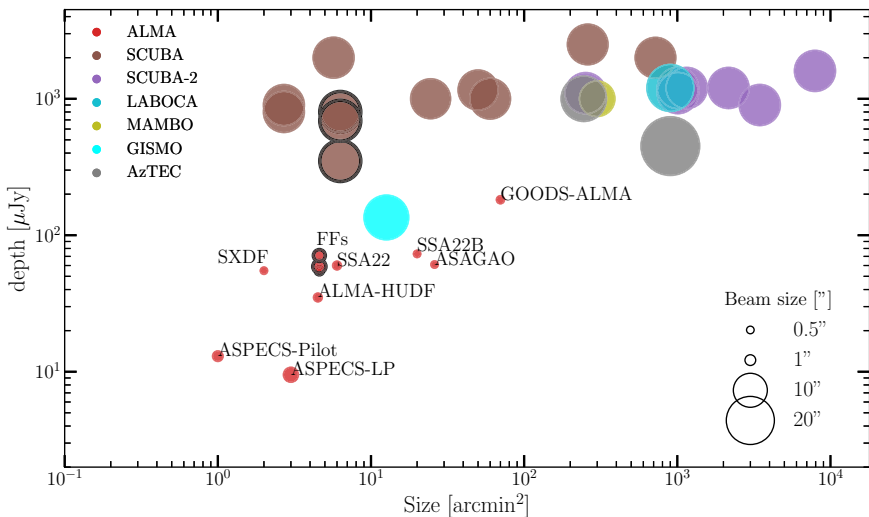**Figure 1.** Size vs. depth for some of the main (sub)millimeter surveys at $850\mu m < \lambda < 3\,mm$. The circles are colour-coded according to the instrument used. The size of the circles corresponds to the size of the beam. The black outer line indicates that the survey covers a lensed area. This list is not exhaustive. We point out that to date, the GOODS-ALMA survey is the largest (sub)millimetre survey without confusion issues. The list of all the surveys shown, all the references, as well as the original figure, can be found in the PhD manuscript of M. Franco.

Since the commissioning of ALMA 8 years ago, several surveys have been obtained, in several regions of the sky The special feature of GOODS-ALMA can be seen clearly in Fig. 1; it is shallower but larger than other ALMA surveys. Thanks to this particularity, we are able to open a different parameter space than other surveys, notably towards massive high redshift star-forming galaxies.

However, it is challenging to obtain large observation areas with ALMA. A mosaic of 846 individual pointings was necessary to create our image. Several other instruments allow us to reach larger areas but at the price of a larger beam. The high angular resolution allows us to avoid blending, to be more confident in the identification of counterparts, to discover optically dark galaxies, and to constrain the sizes of galaxies. This last point, in addition to the computation of the gas mass, SFR, and the depletion time is key to understand galaxy evolution and, in particular, the transition between star-forming and quenched galaxies. We will explore the possibility that these galaxies detected by ALMA are the progenitors of passive elliptical galaxies at $z \sim 2$, which for the moment are largely unknown (e.g., Williams *et al.* 2014; Wang *et al.* 2019), and investigate the evidence we have to assess how this transition is taking place. We assume a Salpeter (1955) Initial Mass Function, and all magnitudes are quoted in the AB system (Oke & Gunn 1983).

## 2. GOODS-ALMA survey

We use ALMA observations (Project ID: 2015.1.00543.S; PI: D. Elbaz), covering 69 arcmin$^2$ within the GOODS-South field (Franco *et al.* 2018). We reach a median rms sensitivity $\sigma \simeq 0.18\,mJy\,beam^{-1}$ in the mosaic tapered to 0.60". We chose to extract sources in this mosaic using two techniques. The first is a blind extraction down to a threshold of 4.8 $\sigma$, which assures us a purity (see Eq. 1 of Franco *et al.* 2018) of 80%. This blind extraction allows us to carry out systematic statistical analysis as well as number counts. This technique also allows us to exploit one of the great strengths of a blind survey - to detect galaxies that had not been detected by other surveys, in particular

in deep fields with Hubble down to a $5\sigma$ limiting depth of H = 28.2 AB (HST/WFC3 F160W), also known as "HST-dark" or "optically dark" galaxies. These galaxies represent 20% (4/20) of our blind detections. We also extended the source detection in the GOODS-ALMA field down to a $3.5\sigma$ threshold using IRAC and the VLA. This allowed us to detect 16 additional galaxies in order to have a more complete view of the galaxies present in this field. The comparison between the number of detected galaxies and the number of galaxies expected by the number counts suggests that we detect more than 70–90% of the galaxies at 1.1 mm with fluxes greater than 0.65 mJy.

## 3. The slow downfall of star-formation in $z = 2-3$ massive galaxies

Thanks to these unique characteristics (large surface area and limited sensitivity compared to other ALMA surveys), GOODS-ALMA allowed us to detect distant and massive galaxies. As these galaxies are rare in terms of surface density, we need to cover large areas to detect them. These galaxies are more massive and more distant than those detected over a smaller surface during the same observation time. We have detected some of the most massive galaxies at $z = 2-4$ (see Fig. 12 in Franco *et al.* 2020a). The vast majority of the sample lie on or in the upper part of the main sequence (MS; e.g., Noeske *et al.* 2007; Elbaz *et al.* 2007; Schreiber *et al.* 2015, see Fig. 4 in Franco *et al.* 2020b). We also note that these galaxies are close to the limit between the power-law MS relation between SFR and stellar mass, and the bending of MS at high stellar mass (Abramson *et al.* 2014; Schreiber *et al.* 2016; Popesso *et al.* 2019).

These galaxies have high SFRs and cannot continue to form stars for long periods at this rate, otherwise we would see at $z \sim 1$, or in the local Universe, galaxies more massive than those we observe now. We are directly observing massive galaxies rapidly producing stars, and we know that in the "near" future (a few hundred million years at most), this rate of star formation may decrease. We therefore have an ideal laboratory to observe this critical period for galaxies, and investigate whether we have enough evidence using ALMA observations and rich multi-wavelength supporting data to determine if a clear scenario emerges for the decline of SFR in these galaxies.

### 3.1. *Low depletion time and low gas fraction*

We have investigated the molecular gas reservoirs of the galaxies detected with ALMA, as well as their depletion times. We extracted key parameters for galaxies with *Herschel* counterparts by constraining their spectral energy distributions using the SED fitting code CIGALE (Code Investigating Galaxies Emission; Boquien *et al.* 2019). We then converted the dust mass (Draine *et al.* 2014 models) into a gas mass using the Leroy *et al.* 2011 relations and the metallicity from Genzel *et al.* (2012). We consider only the galaxies that have *Herschel* counterparts (21 galaxies) in addition to a 1.1mm ALMA detection in order to avoid deriving two physical quantities (infrared luminosity and gas mass) with only one data point.

In order to understand whether our galaxy population has a molecular gas deficit or excess, we compared the gas masses of our galaxies with the relationship presented in Tacconi *et al.* (2018), derived from a large sample of 1444 star-forming galaxies between $z = 0 - 4$. We also compared the depletion times ($\tau_{dep} = M_{gas}/SFR = 1/SFE$, where SFR is the total $SFR = SFR_{IR} + SFR_{UV}$ and SFE is the star formation efficiency). This is the characteristic time a galaxy needs to empty its gas reserves, assuming a constant SFR and no gas replenishment, between our sample and Tacconi *et al.* (2018) (Fig. 2).

For the sake of clarity, we have displayed the Tacconi *et al.* (2018) relation corresponding to the median redshift ($z_{med} = 2.7$) and the median stellar mass ($M_{\star,med} = 8.5 \times 10^{10} M_{\odot}$) of our sample, and re-scaled the gas fraction and the depletion time of each
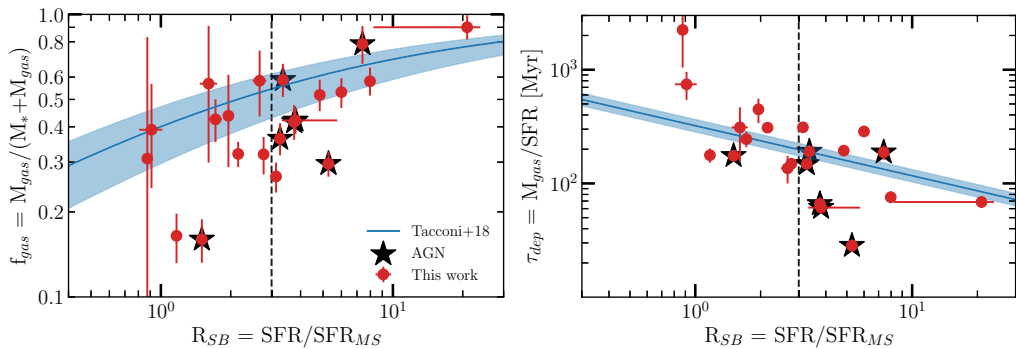
**Figure 2.** Evolution of the molecular gas fraction ($f_{gas}$) and the gas depletion timescale ($\tau_{dep}$) as a function of the distance to the main sequence of star-forming galaxies ($R_{SB} = SFR/SFR_{MS}$) for galaxies detected in the GOODS-ALMA field. The solid blue line shows the relation obtained by Tacconi *et al.* (2018) for the median redshift and stellar mass of our sample. The uncertainty on the mean trend is obtained by Monte-Carlo simulations. In order to compare the gas fractions of all of the galaxies in our sample, we have rescaled our gas fractions according to the median redshift and stellar mass of our sample. Figure from Franco *et al.* (2020b).

galaxy individually to preserve the distance between the galaxy and the Tacconi *et al.* (2018) relation. We investigated whether galaxies hosting an AGN exhibited different characteristics to other galaxies. We used a criterion to discriminate the AGNs based on their X-ray luminosity using the 7Ms Chandra Deep Field-South Survey (Luo *et al.* 2017). The black stars on Fig. 2 represent galaxies with $L_{X,int} > 10^{43}\,\mathrm{erg\,s^{-1}}$.

We recover the global trend of an increase in gas fraction with distance to the main sequence ($R_{SB} = SFR/SFR_{MS}$). Our sample of galaxies exhibits a large scatter in the plane $f_g$- $R_{SB}$. Moreover, we find that a significant part of our sample, approximately (40%), lie below this relation. This is valid for both starburst and MS galaxies.

We also compared the gas depletion time with the Tacconi *et al.* (2018) relation, and find that a significant part of our sample has a low gas depletion time. For both depletion time and gas fraction, we see that galaxies hosting an AGN have, on average, a higher gas fraction and depletion time than galaxies with lower X-ray luminosities.

## 3.2. *Towards a reduction in the size of galaxies*

We determine whether our galaxies, that we see are compact at millimetre wavelengths, are also compact in H-band. Remarkably, we found that for the galaxies for which we have sizes measured in H-band (Van der Wel *et al.* 2014), these H band sizes are on the trend of star-forming galaxies with comparable redshifts and stellar masses (see Fig. 5 in Franco *et al.* 2020b). We note that in our sample, three galaxies are particularly compact in H-band. These three galaxies share a common characteristic - they host an AGN. Comparing galaxy ALMA sizes with H-band sizes, we find that ALMA sizes correlate well with the H-band trend of quenched galaxies with comparable redshifts and stellar masses. If we consider that ALMA traces the dust-obscured star formation, the fact that the ALMA sizes are more compact than the H-band sizes, and that the ALMA sizes match the trend of quenched galaxies, suggests that the dust-obscured star formation is taking place in the core of the galaxies. This process could morphologically transform a galaxy and therefore make it more compact.

## 4. Discussion and Conclusion

We had the opportunity to expand our knowledge of one of the most studied parts of the sky (the GOODS-South field) by adding a new layer - a new wavelength - over this region. The characteristics of the GOODS-ALMA survey allow us to detect a population of very massive star-forming galaxies at $z = 2-4$ ($z_{med} = 2.7$, $M_{\star,med} = 8.5 \times 10^{10} M_\odot$). We investigated their gas reservoirs, their depletion times and their sizes. We show that a significant part of our sample ($\sim 40\%$) exhibits abnormal low gas fractions. With their high star formation rates and without a gas refill mechanism, they will consume their gas reservoirs in a typical time of 100–200 Myrs. The compact submillimetre sizes of our sample are similar to the $H$-band sizes observed for $z \sim 2$ elliptical galaxies with comparable stellar masses, suggesting that they are building their compact bulges. All these different elements lead us to believe that the galaxies detected in the GOODS-ALMA survey are the ideal progenitors of passive compact galaxies at $z \sim 2$. The large fraction of galaxies with short depletion time, low gas fractions among those hosting an AGN, suggest that the AGN, by a starvation process, can prevent the gas refill of these galaxies. The transformation of the gas into the stars of these galaxies can induce a rapid transition between star-forming and passive galaxies, without needing to invoke an additional quenching mechanism.

## References

Abramson, L. E., Kelson, D. D., Dressler, A., *et al.* 2014, *apjl*, 785, 36
Blain, A. W., Smail, I, Ivison, R. J., *et al.* 2002, *Phys. Rep.*, 369, 111
Boquien, M., Burgarella, D., Roehlly, Y., *et al.* 2019, *aap*, 622, 103
Calzetti, D., Armus, L., Bohlin, R. C., *et al.* 2000 *ApJ*, 533, 682
Cowie, L. L., Songaila, A., Hu, E. M., *et al.* 1996, *AJ*, 112, 839
Draine, B. T., Aniano, G., Krause, O., *et al.* 2019, *ApJ*, 780, 172
Elbaz, D., Daddi, E., Le Borgne, D., *et al.* 2007, *A&A*, 468, 33
Franco, M., Elbaz, D., Bethermin, M., *et al.* 2018, *A&A*, 620, 152
Franco, M., Elbaz, D., Zhou, L., *et al.* 2020, ArXiv:2005.03040
Franco, M., Elbaz, D., Zhou, L., *et al.* 2020, ArXiv:2005.03043
Genzel, R., Tacconi, L. J., Combes, F., *et al.* 2012, *ApJ*, 746, 69
Grogin, N. A., Kocevski, D. D., Faber, S. M., *et al.* 2011, *ApJS*, 197, 35
Koekemoer, A. M., Faber, S. M., Ferguson, H. C., *et al.* 2011, *ApJS*, 197, 36
Leroy, A. K., Bolatto, A., Gordon, K., *et al.* 2011, *ApJ*, 737, 12
Luo, B., Brandt, W. N., Xue, Y. Q., *et al.* 2017, *ApJS*, 228, 2
Madau, P. & Dickinson, M. 2014, *araa*, 52, 415
Meurer, G. R., Heckman, T. M., & Calzetti, D. 1999, *ApJ*, 521, 64
Noeske, K. G., Weiner, B. J., Faber, S. M., *et al.* 2007, *ApJ*, 660, 43
Oke, J. B. & Gunn, J. E. 1983, *ApJ*, 266, 713
Pannella, M., Carilli, C. L., Daddi, E., *et al.* 2009, *ApJ*, 698, 116
Popesso, P., Concas, A., Morselli, L., *et al.* 2019, *MNRAS*, 483, 3
Rodighiero, G., Daddi, E., Baronchelli, I., *et al.* 2011, *ApJ*, 739, 40
Salpeter, E. E. 1955, *ApJ*, 121, 161
Schreiber, C., Pannella, M., Elbaz, D., *et al.* 2015, *A&A*, 575, 74
Schreiber, C., Elbaz, D., Pannella, M., *et al.* 2016, *A&A*, 785, 36
Tacconi, L. J., Genzel, R., Saintonge, A., *et al.* 2018, *ApJ*, 853, 179
van der Wel, A., Franx, M., van Dokkum, P. G., *et al.* 2014, *ApJ*, 788, 28
Williams, C. C., Giavalisco, M., Cassata, P., *et al.* 2016, *ApJ*, 780, 1
Wang, T., Schreiber, C., Elbaz, D., *et al.* 2019, *Nature*, 572, 211